2-Hyroxyethyl Cellulose Doped with Glycolic Acid as Solid Biopolymer Electrolytes for Solid-State Proton Battery

Mohd Ikmar Nizam Mohamad Isa, Muhamad Amirullah Ramlli and Nur Ain Bashirah Aniskari

Abstract— Cellulose derivatives have high potential for use as solid biopolymer electrolytes in proton batteries because they are biodegradable, affordable, have good mechanical properties and their ionic conductivity can be enhanced with addition of ionic dopant. In this work, we developed a new type of solid biopolymer electrolytes (SBEs) based on 2-hydroxyethyl cellulose (2HEC) doped with glycolic acid (GA) as an ionic dopant. A solution casting technique was used to prepare the SBEs. The ionic conductivity and structural properties of the SBEs were analyzed using Electrical Impedance Spectroscopy (EIS), Fourier Transform Infrared spectroscopy (FTIR) and an X-ray Diffractometer (XRD). The highest ionic conductivity achieved was 3.80×10^{-4} S cm^{-1} for the sample with 40 wt.% GA content at room temperature. FTIR analysis showed that complexation occurred in the polymer system from the shifting of $vC\text{-}O$ and v_sCOO^- band of 2HEC and GA. FT-IR deconvolution revealed the increasing pattern of percentage free mobile ions with the addition of GA content, which resulting in the high ionic conductivity of the SBE. All SBEs shows amorphous nature as proven in XRD characterization.

Keywords—Free ions, Ionic conductivity, Proton battery, Solid polymer electrolytes.

I. INTRODUCTION

Solid biopolymer electrolytes (SBEs) is one of interesting study in material research for several years. They caught the attentions of many researchers because of the excellent properties of natural polymer to be used in small electrical devices such as batteries, capacitors and many small electronic components. They are mechanically stable, lightweight, environment friendly and has no leakage problem when used as solid electrolyte in all solid-state battery. Usually they are prepared by doping the host polymer with various type of ionic dopant, which can hugely increase the electrical properties of the host polymer [1,2]. Some application that are suitable for use of SBEs are in solid-state batteries, super-capacitors, power windows and many other solid-state electrochemical devices [3-5]. SBEs usually consist of a crystalline phase-that possess a regular structure with immobile ions, and an amorphous phase having no regular structure with mobile ions [6-10]. A few research groups have demonstrated this phenomenon and revealed the biphasic structure of SBEs [11,12].

The arrangement of the polymer molecules greatly affects the physical properties, chemical behaviour and reactivity of the SBEs. In solid state, the movement of ions mostly occurred in the amorphous phase and moving from one site to another by hopping mechanism [13-15]. Proton conducting polymer is a special class of solid electrolytes with hydrogen ions acting as charged carriers, which was first suggested by Rogers and Ubbelohde, in 1950 [16] and many more researchers subsequently [17-19]. The hopping of ions lead to the increase in ionic conductivity of the material. This suggests that there is a close interplay of the structural nature and conductivity in ionic conducting polymer [20-22].

In this work, a new type of SBEs based on 2-hydroxyethyl cellulose (2HEC) doped with glycolic acid were prepared. 2HEC is one of the cellulose derivatives created by means of etherification. This polymer is widely used in cosmetic, latex paints, building materials, cleaning product and even used as an oilfield chemical as a lubricant, along with many other specialty applications [23-25]. Pharmaceuticals also used 2HEC combined with hydrophobic drugs in capsule formation to improve dissolution [26]. 2HEC is a water-soluble polymer that acts as thickener, binder, emulsifier, stabilizer, film former, and exhibits pseudo-plastic solution behaviour, tolerates salts and retains water. As a good sorbent, 2HEC has a good affinity of ions due to the presence of many polar hydroxyl functional groups that can serve as coordination sites for permanent or temporary ion attachment [27-32]. The ionic conductivity of a polymer can be enhanced by introducing a good ionic dopant into the polymer system, which promotes the dissociation of proton (H^+).

GA is a weak acid base that is a naturally occurring material and it is environmentally friendly. Although many

M. I. N. Isa is with the School of Fundamental Science, Universiti Malaysia Terengganu, 21030 Kuala Nerus, Terengganu, Malaysia (Phone: +609 668 3111; fax: +609 669 3608; e-mail: ikmar_isa@umt.edu.my).

M. A. Ramlli is with the School of Fundamental Science, Universiti Malaysia Terengganu, 21030 Kuala Nerus, Terengganu, Malaysia (e-mail: amirullah_ramlli@hotmail.com).

N. A. A. Bashirah is with School of Fundamental Science, Universiti Malaysia Terengganu, 21030 Kuala Nerus, Terengganu, Malaysia (e-mail: a.n.a.bashirah@gmail.com).

reported that ammonium salt is a good ionic dopant, it is interesting to investigate the GA behaviour as an ionic dopant. This is because GA can undergo partial dissociation, which produces proton (H^+) as a dissociated charge together with glycolate anion ($RCOO^-$), and the charged monomer attached to the backbone of GA [33-35] that eventually can enhance the ionic conductivity of the polymer host. In addition, it is also environmentally friendly. Hence, GA was chosen as an ionic dopant to 2HEC for this work. The 2HEC, GA and 2HEC-GA SBEs were characterised using EIS, FT-IR and XRD to investigate its ionic conductivity and structural properties. To the best of our knowledge, there are no published works on the 2HEC-GA SBEs; therefore, it is a great opportunity to investigate the effect of GA on the properties of 2HEC biopolymer.

II. EXPERIMENTAL

A. Materials

2-hydroxyethyl cellulose (2-HEC) was bought from Sigma-Aldrich and Glycolic acid (GA) was from Merck. Distilled water used as solvent and produced in house using cabinet water distiller.

B. Preparation of solid biopolymer electrolyte (SBE)

Firstly, 2HEC solution was prepared by dissolving 2HEC powder in distilled water by magnetically string at room temperature. Then, the 2HEC solution was doped with different GA concentrations (10, 20, 30, 40, 50) wt. % and continue to stir until homogenous. After that, pour the solution into several Petri dishes and dry in oven at 60°C. Completely dried samples were kept in desiccators to prevent moisture contamination. Table 1 lists the sample designation in this work. Sample GA0 was used as reference.

Table 1. Sample designation

Sample	CMC (g)	GA (wt. %)
GA0		0
GA10		10
GA20		20
GA30	2 ± 0.02	30
GA40		40
GA50		50

C. Characterization

The SBEs were characterized using Electrochemical impedance spectroscopy (EIS), Fourier transform infrared (FT-IR) spectroscopy and X-ray diffractometer (XRD).

D. Electrochemical Impedance Spectroscopy (EIS)

The bulk resistance (R_b) of the SBEs were measured using HIOKI 3532-50 LCR Hi-Tester interfaced with a computer in the frequency range from 50Hz to 1M Hz. The measurement setup was depicted in Fig. 1. The ionic conductivity of the SBEs was determined using (1). Here σ is the ionic conductivity, t is the thickness of SBE (cm), R_b is a bulk resistance (Ω), and A is the contact area of the SBE and electrode (cm^2) [2,11].
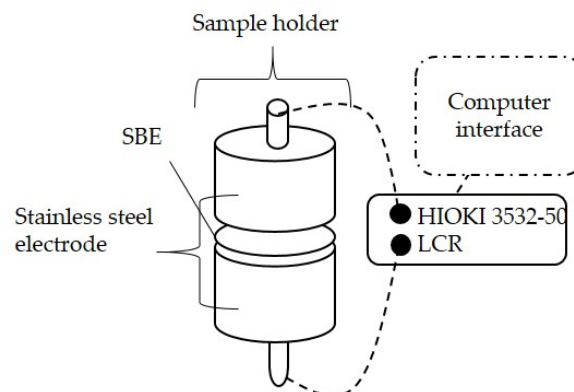

Fig. 1. EIS measurement setup.

$$\sigma = \frac{t}{(R_b A)} \tag{1}$$

E. Fourier Transform Infrared Spectroscopy (FTIR)

A Thermal Nicolet 380 FTIR spectrometer equipped with an Attenuated Total Reflection (ATR) accessory was used to analyze the structure of the SBEs. They were scanned at frequency ranged from 4000 cm^{-1} to 700 cm^{-1} with a resolution of 4 cm^{-1} at ambient temperature.

F. FTIR Deconvolution Technique

Origin 8 fitting software based on the Gaussian-Lorentz function was used to perform the deconvolution technique. The region should be converted into absorbance mode before proceed the deconvolution technique [21, 45]. Percentage of free ions (%) can be calculated using (2). In the equation, A_f is the total area of free ion region and A_c is total area of contact ion region.

$$Percentage\ of\ free\ ions\,(\%) = \frac{A_f}{(A_f + A_c)} \times 100 \tag{2}$$

G. X-ray Diffraction (XRD)

XRD analysis was done by using Ringaku MiniFlex II Diffractometer. Before the scan, 2HEC-GA SBEs were cut into suitable size, and then adhered onto a glass slide before being placed in the sample holder inside the diffractometer. The SBEs were directly scanned at Bragg's angles of 2θ, between 5° and 80° with $CuK\alpha$ source radiation (wavelength =1.5406 Å) at ambient temperature.

III. RESULTS AND DISCUSSION

A. Ionic conductivity

Cole-Cole plots for selected sample GA0 and GA40 (inset) was plotted in Fig. 2. The Cole-Cole plot for GA0 contains two distinctive region, a semicircle and an inclined spike. The semicircle can be related to the SBE being partially resistive and capacitive. However, the semicircle diminished for sample GA40. The reduced semicircle is a sign of increased ionic mobility and the number of free ions in the SBE as well [47]. R_b value was determined from the interception of the semicircle and inclined spike with the Z_r-Axis as shown in Fig. 2.

The calculated value of ionic conductivity was plotted in a graph of ionic conductivity against GA contents (wt. %) and depicted in Fig. 4. The ionic conductivity of 2HEC (GA0) is 3.43×10^{-6} S cm^{-1} at room temperature. From Fig. 2, the ionic conductivity increased steadily from GA0 to GA20. The value then spiked to 2.29×10^{-4} S cm^{-1} for GA30 and reached maximum value at 4.01×10^{-4} S cm^{-1} for GA40. The increase of ionic conductivity can be related to the increased number of free mobile ions in the polymer system. With increased number of free mobile ions, they will increase the chance of ionic conduction to occur in the SBE system, which is a significant factor in enhancing the ionic conductivity of the SBE [44,46]. After GA40, ionic conductivity start to decrease and this was observed for GA50. The decreased could be due to the excess of free ions that start to associates, forming ionic clusters in the SBE system. Early observation shows that GA is a good ionic dopant to 2HEC where it managed to increase the ionic conductivity up to two degrees more. Further elaboration on the number of free mobile were discussed in the FTIR deconvolution technique later in this paper.
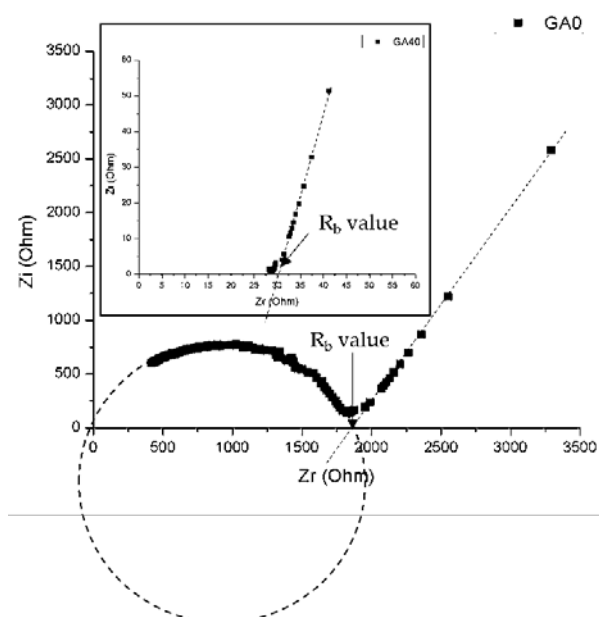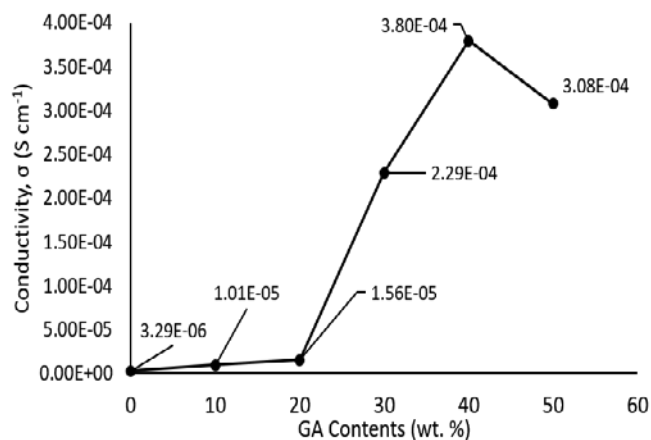

Fig. 3 Ionic conductivity against various GA content

B. FTIR Analysis of Simple Organic Acid

In order to determine the possible interaction between the polymer host and ionic dopant, three different spectra of GA powder, pure 2HEC and 2HEC-GA in a range of 1200-1800 cm^{-1} were plotted in Fig. 4. The incorporation of GA yielded two main absorption features in the 2HEC that are associated with carboxyl group. According to Hay et al. (2007) [36], protonated carboxylic acid (RCOOH) yield absorption band corresponding to carbonyl stretch, $\upsilon C=O$ between 1690 cm^{-1} and 1750 cm^{-1}, and hydroxyl vibration, $\upsilon C-OH$ between 1200 cm^{-1} and 1300 cm^{-1} which comprised of C-O and C-OH group. This vibration often resulted in a single and broad absorption band. According to Cabaniss and McVey, (1995) [37], these changes can be dependent on a few factors, two of which include; i) electron density of carboxyl that was affected by the presence of electron donating or withdrawing functional group; and ii) inter or intra-molecular hydrogen bonding involving a carboxylic oxygen or a proton. These two factors are typically affected more consistently and predictably in the υ_{as} mode relative to the others, making it a useful indicator of structural complexation. However, in this work, the appearance of a υ_{as} peak cannot be observed due to the overlapping of naturally absorbed water band of 2HEC (~1647 cm^{-1}) [46] and the changes are most consistently observed at the υ_s mode of carboxyl group. The coordination of the charged carrier with polar groups in polymer matrix resulted in the complexation and changes in the local structure of host polymer
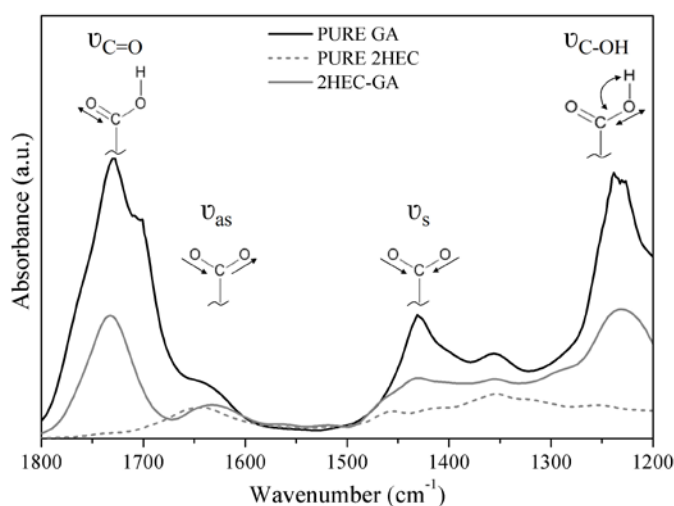

Fig. 2 Cole-Cole plot for GA0 and GA40 (inset)

Fig. 4 FTIR spectra of GA powder, pure 2HEC and GA40 (1200 cm^{-1} – 1800 cm^{-1})

C. FTIR Analysis of 2HEC-GA SBEs

The complexation of GA in 2HEC was observed in FTIR analysis. **Fig. 5** represents the FTIR spectrum of pure 2HEC and 2HEC-GA SBE separated by four region (a) 1150-1350 cm^{-1}, (b) 1500-1800 cm^{-1}, (c) 900-1200 cm^{-1} and (d) 1400-1500 cm^{-1}, respectively. From the figure, the peak intensity for both υC=O and υC-OH of GA in the spectrum of 2HEC-GA SBE experienced a reduction in intensity, which suggested a deprotonation state of GA (dissociation of ions) in the SBE system. The occurrences of new peaks were due to the complexation between the polymer host and ionic dopant.

The absorption bands localized at ~1237 cm^{-1} and ~1730 cm^{-1} are assigned to the stretching vibrations of single and double CO bonds of the carboxylate group of GA, respectively. They are characteristic features of the IR spectrum of GA and they showed increasing intensity with increasing dopant concentration, as expected. In Region c, the peak at ~1055 cm^{-1} is attributed to the υC-O of 2HEC. With the addition of GA, the band shifted to a higher wavenumber at ~ 1086 cm^{-1}. This confirms the complexation of 2HEC and GA in the SBE.

From Region (d), it can be observed that a new peak emerged at ~1440 cm^{-1} for sample GA10, which is believed due to the interactions between 2HEC and GA. The band corresponds to symmetric υ_sCOO,$^-$ which was affected by the increment of GA concentration. With the addition of GA, the band shifted to a lower wavenumber to ~1436 cm^{-1} and the intensity of the peak increased. These significant changes can be associated with the formation of anionic and cationic species through higher dissociation of ionic dopant, thus allowing protonation on 2HEC chain structures. The 2HEC and GA peaks observed in this work are comparable with other works where all the peaks were found at their own specific range [24-32,33,34].
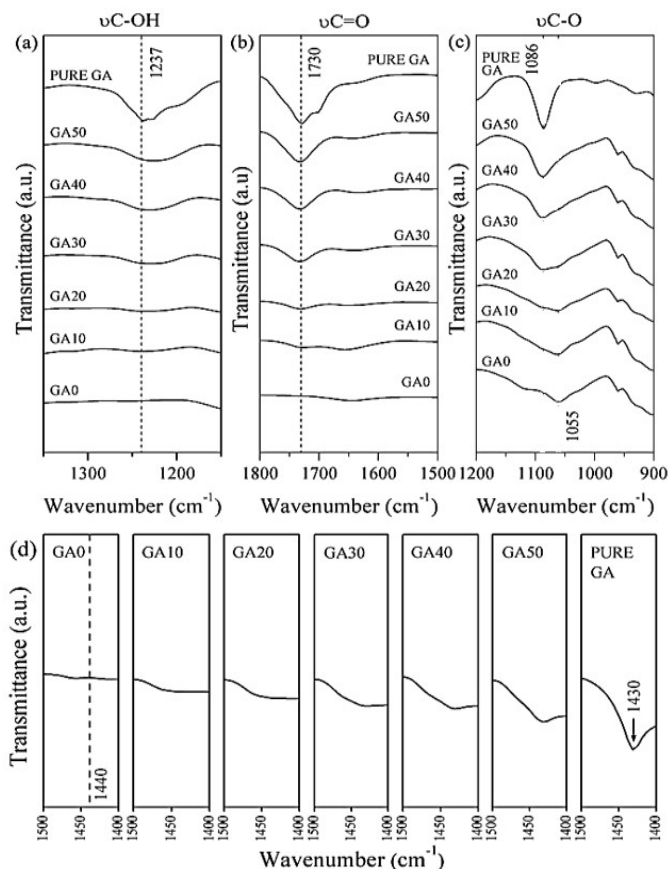

Fig. 5 FTIR spectrum of CMC-GA: (a) 1150 cm^{-1} - 1350 cm^{-1}, (b) 1500 cm^{-1} - 1800 cm^{-1}, (c) 900 cm^{-1} - 1200 cm^{-1} and (d) 1400 cm^{-1} - 1500 cm^{-1} region.

D. FTIR Deconvolution

FTIR deconvolution was performed to isolate the possible peaks presence, intensity change and shifting of the bands, hence further determine the contribution of H$^+$ ions as a charge carrier in 2HEC-GA SBE system [21,22,38]. The deconvolution was based on the Gaussion-Lorentz function and was done using Origin 8 fitting software. The sum of the intensity of all the deconvoluted peaks was ensured to fit the original spectrum where regression value of each peak is approximately unity (R^2 = 0.9998). The deconvolution peaks of υ_sCOO$^-$ were depicted in Fig. 6.

The band representing the free ion can be found at a region between ~1390 cm^{-1} and ~1490 cm^{-1} where the symmetric vibration of carboxylate anion (υ_sCOO$^-$) can be found, which is comparable to work done by Hay & Myneni (2007) [36]. From Fig. 6, the peak located at ~1407 cm^{-1} can be assigned to contact the ions peak, meanwhile the peak at ~1465 cm^{-1} is the C-H characteristic band of 2HEC. It can be observed that peak intensity of glycolate anion increases with increasing GA concentration until reaching the maximum concentration at 40 wt. % and decreased higher concentration.
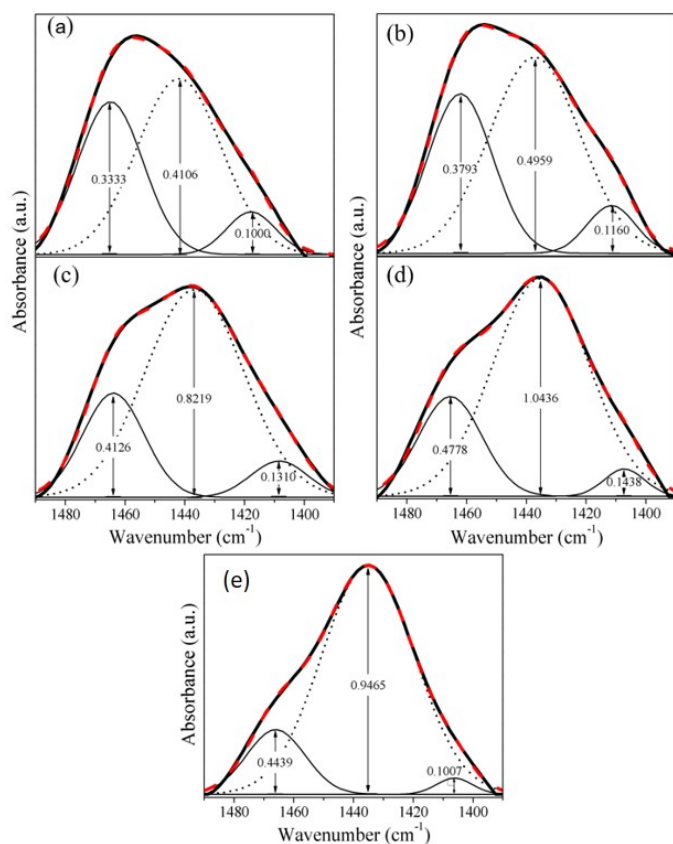
Fig. 6 FTIR deconvolution: (a) GA10, (b) GA20, (c) GA30, (d) GA 40 and (e) GA50 in 1390 cm^{-1} – 1490 cm^{-1}

The increment of the peak indicates the increase of mobile ions with the highest value at 40 % GA concentration, which in agreement in the ionic conductivity analysis performed earlier. The percentage of area of free ions and contact ions were calculated from the ratio of the area of free ions/contact ions to the total area of deconvolution peaks.

Table 2 lists the percentage of free ions in each sample. From the table, it is observed that the percentage of free ions in the SBEs increased until GA40. This specifies that the addition of GA did dissociate more free ions into the polymer system. Whereas at GA50, the percentage of free mobile ions decreased, and it can be due to the ions association that leads to decreased in ionic conductivity of the SBE. The high ionic conductivity of GA40 can be related to its high percentage of free ions where more ionic conduction can occur because the high number of free ions in the system enhanced the ionic conductivity. High contact ion can be related to the ions that associate, hence explains the low ionic conductivity of the SBE [45].

E. XRD analysis

2HEC is a cellulosic material that consists of crystalline and amorphous domains in various proportions [39,43]. The reactivity and chemical behavior are strongly influenced by its structural nature where most of the reactant penetrates only the amorphous regions. It has been reported that cellulose has the most intense reflection peak centered approximately at 2θ = ~22.00°. Fig. 7 shows the X-ray diffractrograms of all SBEs and pure GA. Here, it is observed that the pure GA has multiple crystalline peaks that reveal the crystalline nature of the material. Meanwhile, there are no distinctive crystalline peaks observed in the SBEs, which indicated that GA has completely solvate in the polymer system. In a work done by Attia and Elkader (2013), they reported that the peak attributed to crystalline domain of 2HEC was situated at 2θ = ~22.00°. In this work, pure 2HEC film shows intense reflection peak at ~21.28°, which represent the strongest cellulose peak of the crystalline domain in the polymer host [24]. The broadened cellulose peak with the incorporation of GA can be indicated by the amorphous state of the SBEs.
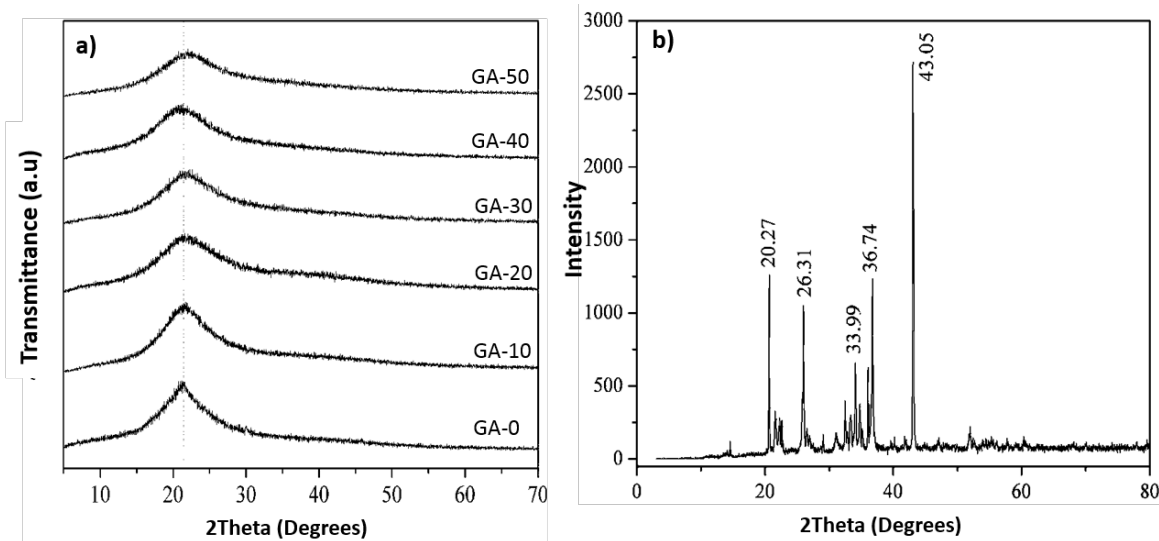

Fig. 7 X-ray pattern for (a) all SBEs, (b) Pure GA

IV. CONCLUSIONS

A new type of SBEs based on 2HEC doped with GA was successfully made via the solution casting technique. The highest ionic conductivity achieved is 3.80×10^{-4} S cm^{-1} for a GA40. The interactions between the host polymer and ionic dopant was revealed from the shifted peaks of υC-O and υC-OH vibration mode. From FT-IR deconvolution analysis, results show that the sample with the highest percentage of free ions has the highest ionic conductivity. This confirms the relations that a high number of free ions helps in increasing the ionic conductivity. X-ray diffraction analysis shows all the SBEs are in an amorphous state with no apparent crystalline peak detected. It can be concluded that GA is an effective ionic dopant because it successfully increased the ionic conductivity of the 2HEC up to two degrees more and shows a promising results to be used as solid electrolyte in solid-state proton battery.

ACKNOWLEDGMENT

REFERENCES

[1] S.B. Aziz; Z.H.Z Abidin, Electrical conduction mechanism in solid polymer electrolytes: New concepts to Arrhenius equation. *Journal of Soft matter*, **2013**, pp. 1-8.

[2] M.N. Chai, M.I.N. Isa, The oleic acid composition effect on the carboxymethyl cellulose based biopolymer electrolyte. *J. Cryst. Process Technol*, **2013**, *3*, pp. 1-4.

[3] P. Kumar, S. Yashonath, Ionic conduction in solid. *J. Chem. Sci.*, **2006**, *118*, pp. 135-154.

[4] S. Rudhziah, M.S.A. Rani, A. Ahmad, N.S. Mohamed, Biopolymer electrolyte based on derivatives of cellulose from kenaf bast fiber. *Polymers*, **2014**, *6*, 2371-pp. 2385.

[5] A.S. Samsudin, M.I.N. Isa, Structural and ionic transport study on CMC doped NH4Br: A new types of biopolymer electrolytes. *Journal of Applied Sciences*, **2012**, *12*, 174-179. Hull, S.; Superionics: Crystal structures and conduction processes. *Rep. Prog. Phys.*, **2004**, *67*, pp. 1233-1314.

[6] D. Ciolacu, L. Pitol-Filho, F. Ciolacu, Studies concerning the accessibility of different allomorphic forms of cellulose. *Cellulose*, **2012**, *19*, pp. 55-68.

[7] D. Ciolacu, V.I. Popa, H. Ritter, Cellulose derivative with adamantoyl group. *J. Appl. Polym. Sci.*, **2006**, *100*, pp. 105-112.

[8] D. Ciolacu, S. Gorgieva, D. Tampu, V. Kokol, Enzymatic hydrolysis of different allomorphic forms of microcrystalline cellulose. *Cellulose*, **2011**, *18*, pp. 1527-1541.

[9] R.C. Agrawal, G.P. Pandey, Solid polymer electrolytes: materials designing and all-solid-state battery applications: an over-view. *J. Phys. D: Appl. Phys.*, **2008**, *41*, pp. 1-18.

[10] K.H. Kamarudin, M.I.N. Isa, Structural and dc ionic conductivity studies of carboxy methylcellulose doped with ammonium nitrate as solid polymer electrolytes. *Int. J. Phys. Sci.*, **2013**, *8*, pp. 1581-1587.

[11] A.S. Samsudin, H.M. Lai, M.I.N. Isa, Biopolymer materials based carboxymethyl cellulose as a proton conducting biopolymer electro-lyte for application in rechargeable battery. *Electrochim. Acta*, **2012**, *129*, pp. 1-13.

[12] M.F.Z. Kadir, Z. Aspanut, S.R. Majid, A.K. Arof, FTIR studies of plasticized poly(vinyl alcohol)-chitosan blend doped with NH4NO3 polymer electrolyte membrane. *Spectrochim Acta A Mol Biomol Spectrosc*, **2011** *78*, pp. 1068-1074.

[13] M.H. Buraidah, A.K. Arof, Characterization of chitosan/PVA blended electrolyte doped with NH4I. *J. Non-Cryst. Solids*, **2011**, *357*, pp. 3261-3266.

[14] S. Ramesh, K.C. Wong, Conductivity, dielectric behavior and thermal stability studies of lithium ion dissociation in poly(methyl methacrylate)-based gel polymer electrolytes. *Ionics*, **2006**, *15*, pp. 249-254.

[15] S.E. Rogers, A.R. Ubbelohde, Melting and crystal structure. III.-low melting acid sulphates. *Transactions of the Faraday Society*, **1950**, *46*, pp. 1051-1061.

[16] E.A. Weiber, S. Takamuku, P. Jannasch, Gufuty Highly proton conducting electrolyte membranes based on poly(arylene sulfone)s with tetrasulfonated segments. *Macromolecules*, **2013**, *46*, pp. 3476–3485.

[17] M. Rikukawa, K. Sanui, Proton-conducting polymer electrolyte membranes based on hydrocarbon polymers. *Prog. Polym. Sci.*, **2000**, *25*, pp. 1463-1502.

[18] P. Simon, Y. Gogotsi, Materials for electrochemical capacitors. *Nat. Mater.*, **2008**, *7*, pp. 845-854.

[19] D. Golodnitskya, E.Straussc, E. Peleda, and S. Greenbaumd, Review-on order and disorder in polymer electrolytes . *J. Electrochem. Soc*, **2015**, *162*, pp. A2551-A2566.

[20] M.H.A. Rahman, M.U. Khanaker, Z.R. Khan, M.Z. Kufian, I.S.M. Noor, and A.K. Arof, Effect of gamma irradiation on poly (vinyledene difluoride)-lithium bis(oxalate)barate electro-lyte. *Phys. Chem. Chem. Phys.*, **2014**, *16*, pp. 11527-11537.

[21] A.K. Arof, S. Amirudin, S.Z. Yusof, and I.M. Noor, A method based on impedance spectroscopy to determine transport properties of polymer electrolytes. *Phys. Chem. Chem. Phys.*, **2014**, *16*, pp. 1856-1867.

[22] Y.N. Sudhakar, M. Selvakumar, and K. D. Bhat, Preparation and characterization of phosphoric acid-doped hydroxyethyl cellulose electrolyte for use in supercapacitors. *Mater. Renew. Sustain. Energy*, **2015**, *4*, pp. 1-9.

[23] G. Attia, and M.F.H. Abd Elkader, Structural, optical and thermal characterization of PVA/2HEC polyblend films. *Int. J. Electrochem. Sci*, **2013**, *8*, pp. 5672-5687.

[24] M. Rosi, F. Iskandar, M.K. Abdullah, Hydrogel-polymer electrolytes based on polyvinyl alcohol and hydroxyethylcellulose for super-capacitor applications. *Int J Electrochem Sci*, **2014**, *9*, pp. 4251-4256.

[25] J. Wang, P. Somasundaran, Mechanisms of ethyl(hydroxyethyl) cellulose–solid interaction: Influence of hydrophobic modification. *J. Colloid Interface Sci.*, **2006**, *293*, pp. 322–332.

[26] M.A. El-Sheikh, S.M. El-Rafie, E.S. Abdel-Halim, and M.H. El-Rafie, Green synthesis of hydroxyethyl cellulose-stabilized silver nanoparticles. *Journal of Polymers*, **2013**, pp. 1-11.

[27] A. Elidrissi, S. El barkany, H. Amhamdi, and A. Maaroufi, Elobaration of the new cellulose derivative films (HECA) based on "Stipa Tenacissima" cellulose of Eastern Morrocco. *J. Mater. Environ. Sci.*, **2010**, *3*, pp. 197-204.

[28] S.K. Kua, C.Y. Chan, Y.Y. Lim, Y.K. Leong, Flow behavior of titanium dioxide dispersions in the presence of 2-hydroxyethyl cellulose. *Colloid Polym. Sci.*, **2000**, *278*, pp. 485-489.

[29] Y. Seki, A. Altinisik, B. Demircioğlu, and C. Tetik, Carboxymethylcellulose (CMC)-hydroxyethylcellulose (HEC) based hydrogels: synthesis and characterization. Cellulose, **2014**, 21, pp. 1689-1698.

[30] S. Himmelein, V. Lewe, M.C.A. Stuart, and B.J. Ravoo, A carbohydrate-based hydrogel containing vesicles as responsive non-covalent cross-linkers. *Chem. Sci.*, **2014**, *5*, pp. 1054-1058.

[31] J.T. Lo, H.T. Yen, C.C. Tsai, B. Chen, S.S. Hou, Interaction between hydrophobically modified 2-hydroxyethyl cellulose and sodium dodecyl sulfate studied by viscometry and two-dimensional NOE NMR spectroscopy. *J. Phys. Chem. B*, **2014**, *118*, pp. 6922-6930.

[32] G. Kister, G. Cassanas, M. Vert, Morphology of poly(glycolic acid) by IR and Raman spectroscopies. *Spectrochim. Acta Mol. Biomol. Spectrosc.*, **1997**, 53, pp. 1399-1403.

[33] Y. Sheena Mary, S. Suprabhan, H.M. Varghese, C.Y. Panicker, IR, Raman and Ab-initio calculations of glycolic acid. *Orient. j chem.*, **2011**, *27*, pp. 215-220.

[34] I. Borukhov, D. Andelman, R. Borrega, M. Cloitre, L. Leibler, and H.Orland, Polyelectrolyte titration: Theory and experiment. *J. Phys. Chem. B*, **2000**, *104*, pp. 11027-11034.

[35] M.B. Hay, and S.C.B. Myneni, Structural environmental of carboxyl groups in natural organic molecules from terrestrial systems. Part 1: Infrared spectroscopy. *Geochim. Cosmochim.*, **2007**, *71*, pp. 3518-3532. http://dx.doi.org/

[36] S.E. Cabaniss, and I.F. McVey, Aqueous infrared carboxylate absorbances: aliphatic monocarboxylates. *Spectrochim. Acta Mol. Biomol. Spectrosc.*, **1995**, 51, pp. 2385–2395.

[37] S.E. Cabaniss, J.A. Leenheer, and I.F. McVey, Aqueous infrared carboxylate absorbances: aliphatic di-acids. Spectrochim. Acta Mol. Biomol. Spectrosc, **1998**, 54, pp. 449-458.

[38] J.K. Kauppinen, D.J. Moffatt, H.H. Mantsch, D.G. Cameron, Fourier self-deconvolution: A method for resolving intrinsically overlapped bands. *Appl. Spectrosc.*, **1982**, *35*, pp. 271-276.

[39] M.K.D. Rambo, and M.M.C. Ferreira, Determination of cellulose crystallinity of banana residues using near infrared spectroscopy and multivariate analysis. *J. Braz. Chem. Soc.*, **2015**, *26*,

[40] M. Hemaa, S. Selvasekarapandian, G. Hirankumar, A. Sakunthala, D. Arunkumara, and H. Nithyaa, Laser Raman and AC impedance spectroscopic studies of PVA: NH4NO3 polymer electrolyte. Spectrochim. Acta Mol. Biomol. Spectrosc., **2010**, *75*, pp. 474–478.

[41] M.I.H. Sohaimy, M.I.N. Isa, Conductivity and Dielectric Analysis of Cellulose Based Solid Polymer Electrolytes Doped with Ammonium Carbonate. *AMM*, **2015**, *719-720*, pp. 67-72.

[42] D. Ciolacu, F. Ciolacu, and V.I. Popa, Amorphous Cellulose-Structure and Characterization. *Cellulose Chemistry and Technology*, **2011**, 45, pp. 13-21.

[43] M.A. Ramlli, and M.I.N. Isa, Solid Biopolymer Electrolytes Based Carboxymethyl Cellulose Doped With Ammonium Fluoride: Ionic Transport and Conduction Mechanism. *Polymers from Renewable Resources*, **2015**, *6*, pp. 55-63.

[44] M.A. Ramlli, and M.I.N. Isa, Structural and Ionic Transport Properties of Protonic Conducting Solid Biopolymer Electrolytes Based on Carboxymethyl Cellulose Doped with Ammonium Fluoride. *J. Phys. Chem. B*, **2016**, *120*, pp. 11567−11573.

[45] M.N. Hafiza, and M.I.N. Isa, Solid polymer electrolyte production from 2-hydroxyethyl cellulose: Effect of ammonium nitrate composition on its structural properties. *Carbohydr Polym.*, **2017**, *165*, pp. 123-131.

[46] N.H. Ahmad, and M.I.N. Isa, Proton conducting solid polymer electrolytes based carboxymethyl cellulose doped ammonium chloride: Ionic conductivity and transport studies. *International Journal of Plastics Technology*, **2015**, *18(2)*, pp. 1-11.